

Search for the radiative decay $\eta \rightarrow \pi^0 \gamma \gamma$ in the SND experiment at VEPP-2M

M. N. Achasov, K. I. Beloborodov, A. V. Berdyugin, A. V. Bozhenok,
 A. G. Bogdanchikov, D. A. Bukin, S. V. Burdin, T. V. Dimova,
 A. A. Drozdetsky, V. P. Druzhinin, D. I. Ganyushin, V. B. Golubev,
 V. N. Ivanchenko, I. A. Koop, A. A. Korol, S. V. Koshuba,
 A. V. Otboev, E. V. Pakhtusova, A. A. Salnikov, V. V. Shary,
 S. I. Serednyakov, Yu. M. Shatunov, V. A. Sidorov, Z. K. Silagadze *,
 A. G. Skripkin, A. A. Valishev, A. V. Vasiljev and Yu. S. Velikzhanin

Budker Institute of Nuclear Physics and
 Novosibirsk State University, 630 090, Novosibirsk, Russia

Abstract

The $\eta \rightarrow \pi^0 \gamma \gamma$ decay was investigated by the SND detector at VEPP-2M e^+e^- collider in the reaction $e^+e^- \rightarrow \phi \rightarrow \eta \gamma$. Here we present the results and some details of this study. We report an upper limit (90% c.l.) $Br(\eta \rightarrow \pi^0 \gamma \gamma) < 8.4 \times 10^{-4}$ as our final result. Our upper limit does not contradict the earlier measurement by GAMS spectrometer. To facilitate future studies a rather detailed review of the problem is also given.

1 Introduction

The experimental history of the $\eta \rightarrow \pi^0 \gamma \gamma$ decay begins in 1966 when 1.2 GeV/c momentum π^- beam from CERN proton synchrotron was used to produce η mesons on a hydrogen target via charge exchange reaction

$$\pi^- + p \rightarrow \eta + n. \quad (1)$$

η meson was tagged by means of neutron time-of-flight measurement. The γ -ray emission spectrum from the subsequent η decays was measured by a lead glass Cherenkov counter. As it was claimed in Ref.[1], the observed γ -ray spectrum could not be explained by $\eta \rightarrow 2\gamma$ and $\eta \rightarrow 3\pi^0$ decay

*Corresponding author, e-mail silagadze@inp.nsk.su

modes only. An equally intensive $\eta \rightarrow \pi^0\gamma\gamma$ decay was required to get a good approximation of the measured spectrum.

The next experiment carried out in Brookhaven [2] utilized a similar technique except for an order of magnitude higher incident π^- beam momentum and a spark chamber as a γ -ray detector. No $\eta \rightarrow \pi^0\gamma\gamma$ signal was observed in the collected 4γ events.

That was the beginning of the $\eta \rightarrow \pi^0\gamma\gamma$ decay puzzle which lasted for the next 15 years. Several other experiments were performed during this time [3 ÷ 13], but the situation still remained unclear. The results of these experiments are shown in Fig.1. For experiments that did not measure this branching ratio directly we calculated it using their results and current PDG table values for $\text{Br}(\eta \rightarrow 2\gamma) = (39.21 \pm 0.34)\%$ and $\text{Br}(\eta \rightarrow \text{neutrals}) = (71.5 \pm 0.6)\%$.

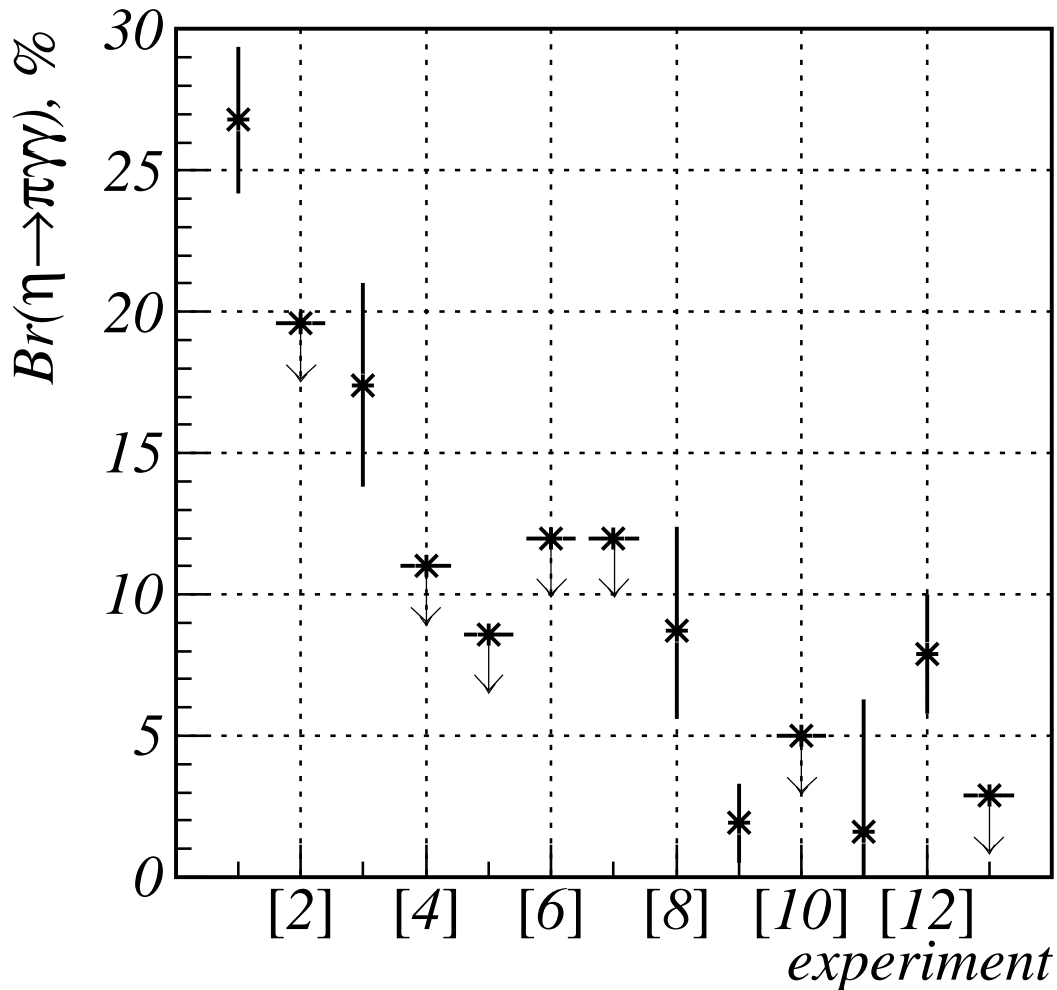


Figure 1: The history of the $\eta \rightarrow \pi^0\gamma\gamma$ decay measurements up to 1980.

In many experiments the reaction (1) with rather low π^- momentum

~ 1 GeV/c was used as a source of η mesons and optical spark chambers as γ -ray detectors, as in [2]. Rather low detection efficiency for photons lead to a severe background from intense $\eta \rightarrow 3\pi^0$ decay. This was clearly demonstrated in [11]. It is interesting to note, however, that despite the authors' firm conclusion that all observed 4γ events in the η peak were likely from the $\eta \rightarrow 3\pi^0$ decay they presented an odd $\Gamma(\eta \rightarrow \pi^0\gamma\gamma) = (1.6 \pm 4.7)\% \Gamma(\eta \rightarrow \text{neutrals})$ as their final result rather than just an upper limit. We mention this curious fact here only to show how great is sometimes the pressure of previously published results — a source of biases in high energy physics experiments not always appreciated.

High γ detection efficiency provided by heavy liquid bubble chamber techniques was also used in $\eta \rightarrow \pi^0\gamma\gamma$ decay studies. For example, for a xenon bubble chamber an average γ detection efficiency was as high as 94% [12]. In this experiment, the chamber was irradiated by a 2.34 GeV/c π^+ beam and η mesons were produced on quasi-free neutrons in the xenon nuclei through the reaction $\pi^+ + n \rightarrow \eta + p$. Experiment [13] also used a xenon bubble chamber but $\pi^- + n \rightarrow \pi^- + n + \eta$ reaction to produce η -s by an incident 3.5 GeV/c π^- beam. A variation of this technique, a hydrogen target inside a heavy freon (CF_3Br) bubble chamber, was used in [6, 7] with the η meson production reaction $\pi^+ + p \rightarrow \pi^+ + p + \eta$. It was again emphasized in [7] that the experimental difficulty in the $\eta \rightarrow \pi^0\gamma\gamma$ decay studies comes essentially from the $\eta \rightarrow 3\pi^0$ background.

Let us mention also two other bubble chamber experiments, for completeness. In [8], $0.7 \div 0.8$ GeV/c K^- beam at BNL Alternate Gradient Synchrotron (AGS) facility was used to produce η mesons in a hydrogen bubble chamber via reaction $K^- + p \rightarrow \Lambda + \eta$. In [4] the $\pi^+ + d \rightarrow p + p + \eta$ reaction in a bubble chamber filled with liquid deuterium was used, 0.82 GeV/c π^+ beam provided also by AGS.

These bubble chamber experiments also produced controversial results. A real breakthrough in the field occurred in 1981 with GAMS experiment at Serpukhov [14]. The η mesons were produced again via the charge exchange reaction (1). But now the incident π^- beam momentum was 38 GeV/c. This incident energy increase dramatically improved the $\eta \rightarrow 3\pi^0$ background suppression. In previous experiments low energy (~ 1 GeV) η -s were used, which means relatively high thresholds for γ -ray detection. So two softest γ -rays could easily escape unnoticed, and this is one possible mechanism for $\eta \rightarrow 3\pi^0$ decay to mimic the desired $\eta \rightarrow \pi^0\gamma\gamma$ decay. With increasing η energies, relative threshold for γ -ray detection gets lower, and

so does the $\eta \rightarrow 3\pi^0$ background. There is also another benefit of higher energies: higher invariant mass resolution of the detector for higher photon energies significantly improves suppression of the background. An order of magnitude lower upper limit $\text{Br}(\eta \rightarrow \pi^0\gamma\gamma) < 0.3\%$ (at 90% confidence level) was reported by this experiment.

In the next run of the same GAMS experiment a lower π^- momentum 30 GeV/c was used. But because of improvements in the detector and accelerator performance significantly higher statistics was collected: about 6×10^5 η mesons produced via the charge exchange reaction (1). At last the $\eta \rightarrow \pi^0\gamma\gamma$ decay was discovered with certainty [15]. In the mass spectrum of the $\pi^0\gamma\gamma$ system a narrow η peak was observed over a smooth background caused by the $\eta \rightarrow 3\pi^0$ decay. The statistical significance of the effect was greater than seven standard deviations. The measured branching ratio was

$$\text{Br}(\eta \rightarrow \pi^0\gamma\gamma) = (9.5 \pm 2.3) \times 10^{-4}.$$

After about two years the same experimental statistics was reanalyzed with improved reconstruction program for γ -rays from the showers in the GAMS spectrometer [16]. The improvement provided better treatment of overlapping showers and allowed to reduce the background further. The new result was [16, 17]

$$\text{Br}(\eta \rightarrow \pi^0\gamma\gamma) = (7.1 \pm 1.4) \times 10^{-4}. \quad (2)$$

Now some words on history of theoretical studies of the $\eta \rightarrow \pi^0\gamma\gamma$ decay. To our knowledge, the first estimate of this decay rate was given by Okubo and Sakita in [18]. They assumed that the following effective coupling

$$\mathcal{L}_{eff} = \xi F_{\mu\nu} F^{\mu\nu} \eta \pi^0 \quad (3)$$

was responsible for the decay. To estimate the value of the coupling constant ξ , they further assumed that the interaction (3) was also the source of the η - π^0 transition mass through the tadpole diagram which one obtains by contracting photon lines in the $\eta\pi^0\gamma\gamma$ interaction vertex. The η - π^0 transition mass itself was estimated by using the unitary symmetry inspired mass formula. This approach was hampered by the fact that the tadpole diagram is badly divergent and one needs some cut-off to calculate its strongly cut-off dependent value. By taking the cut-off at the nucleon mass, they obtained $\Gamma(\eta \rightarrow \pi^0\gamma\gamma) \sim 8$ eV. But the authors admitted that this estimate may easily be wrong by an order of magnitude. For comparison, the experimental result (2) implies $\Gamma(\eta \rightarrow \pi^0\gamma\gamma) = 0.84 \pm 0.18$ eV.

After some years, it was shown in [19] that vector meson dominance model (VDM) with trilinear meson interactions of the VVP and VPP type, previously successfully applied to the $\eta \rightarrow \pi^+\pi^-\gamma$ and $\eta \rightarrow \gamma\gamma$ decays [20], predicts too small ($\sim 10^{-3}$) ratio of the $\eta \rightarrow \pi^0\gamma\gamma$ and $\eta \rightarrow \gamma\gamma$ decay widths, indicating $\Gamma(\eta \rightarrow \pi^0\gamma\gamma) \sim 0.5$ eV. So it became clear that a large rate for the $\eta \rightarrow \pi^0\gamma\gamma$ decay, which was reported by several experiments at that time, caused some theoretical embarrassment. As a possible way out Singer suggested in [21] a rather strong quadrilinear VVPP meson interaction which can be dominating in the $\eta \rightarrow \pi^0\gamma\gamma$ decay. The VDM model was further examined by Oppo and Oneda in [22]. It was confirmed that this model predicts a small $\eta \rightarrow \pi^0\gamma\gamma$ decay width in the 0.3–0.6 eV range. But the authors also indicated a possible additional contribution coming from a scalar meson intermediate state. There was very little experimental knowledge about scalar mesons at that time (even nowadays scalar mesons still remain the most experimentally unsettled question in the low energy phenomenology). Using chiral symmetry arguments Gounaris [23] estimated scalar meson contribution and obtained $\Gamma(\eta \rightarrow \pi^0\gamma\gamma) = 1.0 \pm 0.2$ eV in excellent agreement with the present experimental result (2). But this correct experimental result then had years ahead to come. So the Gounaris' result was considered as a failure of the theory rather than success. Some theoretical work followed [24, 25, 26] which seemed successful in producing large enough decay width by using essentially scalar meson contribution. The new experimental situation [14, 15], however, promptly depreciated all such attempts and stopped them forever.

Meanwhile it became increasingly evident that the chiral symmetry and its spontaneous breaking play crucial role in the low energy hadron phenomenology. This was culminated by creating a theoretical framework called chiral perturbation theory [27] where the degrees of freedom used are the low-lying hadron states instead of useless in the low energy world (current) quarks and gluons. The situation here resembles [28] theory of superconductivity: nobody questions the QED as underlying theory of all electromagnetic phenomena, but it does not help much while dealing with superconductivity. The reason is that electrons and photons are not adequate degrees of freedom for the superconductive phase. The translational symmetry is spontaneously broken due to presence of atomic lattice. The resulting Goldstone bosons (phonons) mediate the most important interactions. Electron gets a dynamical mass and becomes quite different from the electron of the bare QED Lagrangian. In the case of chiral perturbation

theory (ChPT), the Goldstone bosons, associated with the spontaneous breaking of the chiral symmetry, are pseudoscalar mesons. So their interactions can be predicted to a great deal in the low energy limit. Therefore it is not surprising that the last chapter of our theoretical history is related to ChPT.

But at first let us mention some before-ChPT-age papers, for completeness. It was shown in [29, 30] that, unlikely to $\eta \rightarrow \gamma\gamma$ decay, baryon loop contribution vanishes for the $\eta \rightarrow \pi^0\gamma\gamma$ decay in the chiral symmetry limit. Pion loop contribution turned out to be very small [30]. Failing to find any large contribution in the $\eta \rightarrow \pi^0\gamma\gamma$ decay rate in otherwise successful chiral model, the authors of [30] suggested that something may be wrong with the experiment itself and soon the GAMS experiment showed that they were correct. Right after this crucial experiment two papers appeared [31, 32] which calculated the $\eta \rightarrow \pi^0\gamma\gamma$ decay width by using (constituent) quark loops to estimate various meson amplitudes. They obtained the correct magnitude of the decay width ~ 1 eV.

In ChPT the $\eta \rightarrow \pi^0\gamma\gamma$ decay was studied in [33]. This decay is rather peculiar from the point of view of the chiral perturbation theory. In the momentum expansion, the leading $O(p^2)$ term is absent because there is no direct coupling of photons to π^0 and η . Due to the same reason the $O(p^4)$ tree contribution is also absent. So for the $\eta \rightarrow \pi^0\gamma\gamma$ decay ChPT series starts with $O(p^4)$ one-loop contributions. But these loop contributions are also very small. Usually dominant pion loops are suppressed here because they contain G-parity violating $\eta\pi^+\pi^-\pi^0$ vertex. Kaon loops, although not violating G-parity, also give negligible contribution because of large kaon mass. It turned out that the main contribution comes from $O(p^6)$ counterterms which are needed in ChPT to cancel various divergences. The coefficients of these counterterms are not determined by the theory itself and should be fixed either from experimental information or by assuming that they are saturated by meson resonances (vector meson exchange giving the dominant contribution). In [33] the latter approach was adopted which gave $\Gamma(\eta \rightarrow \pi^0\gamma\gamma) \approx 0.18$ eV — too small compared to the experimental value (2). But, as was argued in [33], keeping momentum dependence in the vector meson propagators gives an “all-order” estimate (that is $O(p^6)$ and higher) of the corresponding contribution of about 0.31 eV, in agreement with the old VDM prediction [19, 22]. Note that although the kaon loop amplitude alone is totally insignificant, its interference with the “all-order” VDM amplitude gives still small but noticeable contribution [34].

There are also scalar and tensor meson contributions (which signs cannot be unambiguously determined) and one-loop contribution at $O(p^8)$ which is of the same order of magnitude as the $O(p^4)$ contribution, because it does not violate G-parity. Taking into account all these mechanisms, the final estimate of [33] was

$$\Gamma(\eta \rightarrow \pi^0 \gamma \gamma) = 0.42 \pm 0.20 \text{ eV}. \quad (4)$$

Some more details were given in [35] but the result essentially remained unchanged. Contributions of the C-odd axial vector resonances were considered in [36]. These contributions increase (4) by about 10%. But this is still not enough to reconcile the ChPT result (4) with the experiment. Therefore it was suggested in [37] that the resonance saturation assumption may not be valid for $O(p^6)$ chiral Lagrangian (although it works quite well at $O(p^4)$). Some indications about validity of this suggestion is provided by Bellucci and Bruno in [38]. They calculated the coefficients of the $O(p^6)$ counterterms in the framework of the Extended Nambu Jona-Lasinio model (ENJL) and obtained

$$\Gamma(\eta \rightarrow \pi^0 \gamma \gamma) = 0.58 \pm 0.3 \text{ eV}.$$

It is higher than (4) and is in agreement with experiment within one standard deviation. However, the same coefficients when calculated by using another chiral effective Lagrangian, obtained by a bosonization of the NJL model, led [39] to small decay width of the order of 0.1 eV, while the $\gamma \gamma \rightarrow \pi^0 \pi^0$ experimental data were reproduced well. Another analysis [40] within the ENJL model framework also produced rather small $O(p^6)$ rate in the leading $1/N_c$ approximation

$$\Gamma(\eta \rightarrow \pi^0 \gamma \gamma) = (0.27_{-0.07}^{+0.18}) \text{ eV}.$$

On the contrary, Nemoto et al. argued [41] that the ENJL model might be quite successful in explaining experimental $\eta \rightarrow \pi^0 \gamma \gamma$ width if one includes instanton induced 6-quark interactions, which lead to a strong $U_A(1)$ breaking and nonstandard η - η' mixing angle close to zero.

As we have seen, $\eta \rightarrow \pi^0 \gamma \gamma$ decay has dramatic, both experimental and theoretical, history. And the story is by no means over yet. From the theoretical point of view, this decay provides unique possibility to probe higher order effects in ChPT. But at present these effects can not be calculated without model ambiguities. And the situation will hardly change

until more precise and detailed experimental data appear. Such data about $\eta \rightarrow \pi^0 \gamma \gamma$ decay are also highly desirable for understanding other interesting rare decays, such as $K_L \rightarrow \pi^0 e^+ e^-$ [42] (in which, it is believed, a signal of the direct CP-violation can be observed) and $\eta \rightarrow \pi^0 l^+ l^-$ [43, 44, 45] (which is a sensitive probe of C-conservation in the electromagnetic interaction of hadrons). Despite considerable experimental effort, only one reliable measurement of the $\eta \rightarrow \pi^0 \gamma \gamma$ decay rate exists at present. Therefore [46], “a re-measurement of the decay rate and a measurement of the decay distributions is certainly desirable”.

2 Detector and experiment

The SND detector (Fig.2) is a general purpose nonmagnetic detector which successfully operates at the VEPP-2M collider [47] since 1995. The detailed description of this detector and some of its subsystems can be found elsewhere [48, 49, 50], and will be not repeated here. But maybe it is worthwhile to mention some features of the SND calorimeter, because this subsystem is crucial in the analysis like one presented in this article. The SND calorimeter consists of 1630 NaI(Tl) crystals with a total weight of 3.6 tons. Crystals are assembled in three spherical shells with solid angle coverage $\sim 90\%$ of 4π . Each calorimeter layer includes 520–560 crystals of eight different shapes. The total thickness of the calorimeter is $13.5X_0$ (35 cm) of NaI(Tl).

The calorimeter was calibrated by using cosmic muons [51] and $e^+e^- \rightarrow e^+e^-$ Bhabha events [52]. The dependence of the calorimeter energy resolution on photon energy is shown in Fig.3. This dependence can be fitted as:

$$\frac{\sigma_E}{E}(\%) = \frac{4.2\%}{\sqrt[4]{E(\text{GeV})}}.$$

Several effects influence the energy resolution, such as passive material before and inside the calorimeter, leakage of shower energy through the calorimeter, electronics instability and calibration inaccuracy, light collection nonuniformity over the crystal volume. Reasonably good agreement between simulated and measured energy resolutions was achieved after all these effects were duly taken into account in the simulation. An average energy deposition for photons in the calorimeter is about 93% of their initial energy.

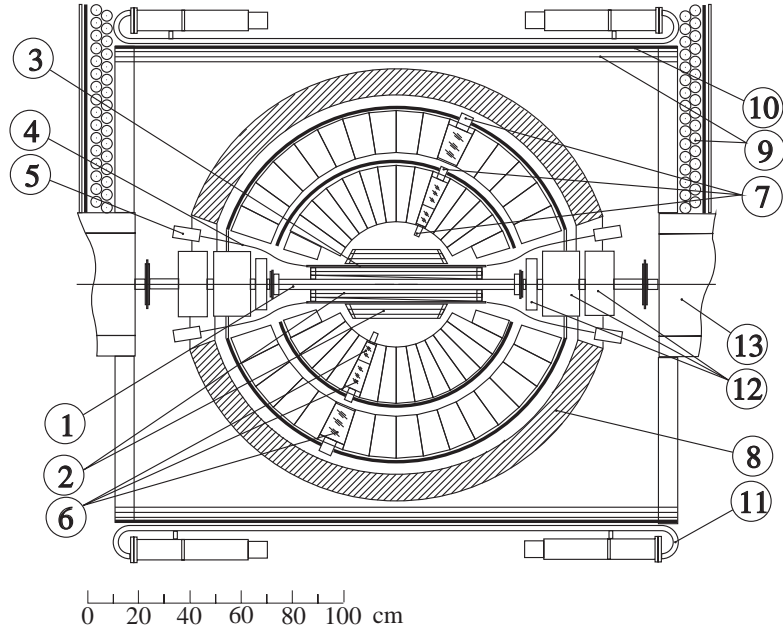


Figure 2: SND detector, section along the beams: (1) beam pipe, (2) drift chambers, (3) scintillation counter, (4) light guides, (5) PMTs, (6) NaI(Tl) crystals, (7) vacuum phototriodes, (8) iron absorber, (9) streamer tubes, (10) 1 cm iron plates, (11) scintillation counters, (12) and (13) elements of collider magnetic system.

High granularity of the calorimeter ensures rather good angular resolution for photons. A novel method for reconstruction of photon angles was suggested in [53]. It is based on an empirical finding that the distribution function of energy deposition outside the cone with the angle θ around the shower direction has the following form for electromagnetic showers in the SND calorimeter (according to simulation)

$$E(\theta) = \alpha \cdot \exp(-\sqrt{\theta/\beta}), \quad (5)$$

where the α and β parameters turned out to be practically independent of the photon energy over the interval $50 \div 700$ MeV. Fig.4 shows the calorimeter angular resolution as a function of photon energy. This energy dependence can be approximated as

$$\sigma_\varphi = \frac{0.82^\circ}{\sqrt{E(\text{GeV})}} \oplus 0.63^\circ.$$

High granularity also enables to discriminate merged photons in the calorimeter by examining energy deposition profile of the corresponding electromagnetic shower in transverse direction. Merging of photons is the main mechanism for $\eta \rightarrow 3\pi^0$ decays to imitate the desired $\eta \rightarrow \pi^0\gamma\gamma$

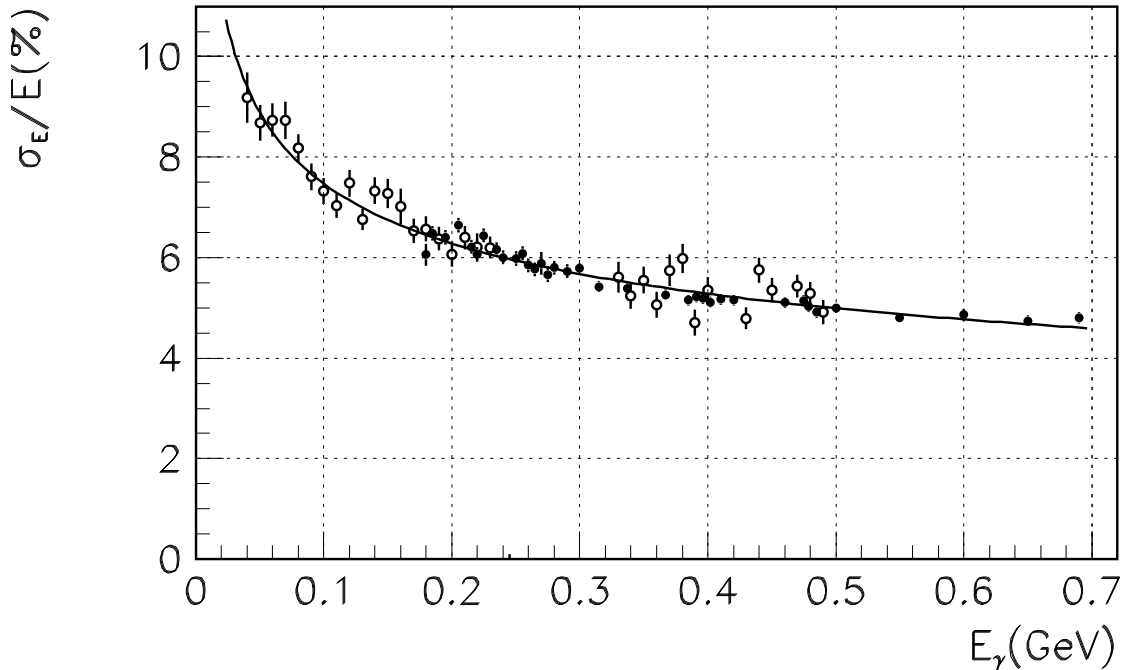


Figure 3: Calorimeter energy resolution versus photon energy. Energy resolution was measured by using $e^+e^- \rightarrow \gamma\gamma$ (dots) and $e^+e^- \rightarrow e^+e^-\gamma$ (circles) reactions.

process (another one is a loss of photons through openings in the calorimeter). So, for background suppression, it is very important to recognize merged photons. In [54] a parameter was suggested to separate hadronic and electromagnetic showers in the SND calorimeter by comparison of actual transverse energy profile of the shower with the expected one (5) for a single photon. The same parameter also helps to discriminate merged photons.

The results presented in this article are based on the statistics collected by SND in two experiments. The first one was carried out in the time period from February 1996 until January 1997. Seven successive scans were performed in the center of mass energy range from 980 to 1044 MeV. Data were recorded at 14 different beam energy points. Collected statistics was almost tripled during the next experiment in 1997–1998. It consisted of three scans at 16 energy points in the interval from 984 to 1060 MeV. The total integrated luminosity used in this work is equal to 12.2 pb^{-1} and corresponds to about 2×10^7 ϕ mesons produced. The corresponding number of η mesons from $\phi \rightarrow \eta\gamma$ decay is 2.58×10^5 . The collider luminosity was measured using the process $e^+e^- \rightarrow 2\gamma$. Systematic error of the luminosity measurement estimated using $e^+e^- \rightarrow e^+e^-$ reaction is close to 3%.

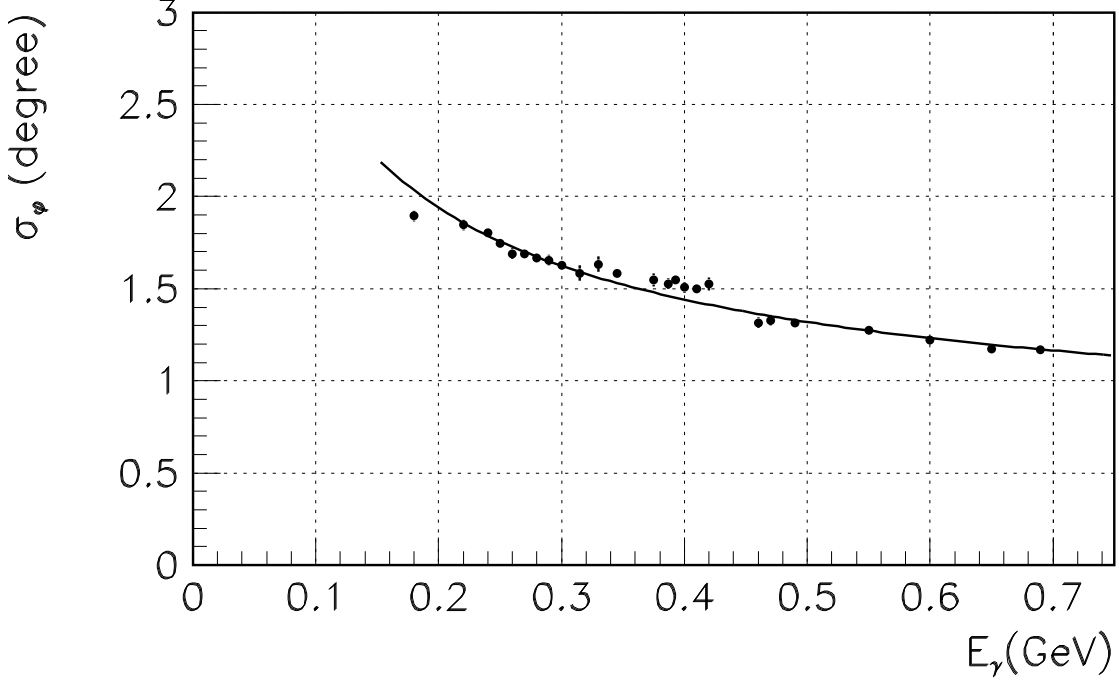


Figure 4: Calorimeter angular resolution versus photon energy.

3 Theoretical models for Monte Carlo simulation

The general form of the $\eta(p) \rightarrow \pi^0(q)\gamma(k_1, \epsilon_1)\gamma(k_2, \epsilon_2)$ transition amplitude as a function of particle momenta and photon polarization vectors is dictated by gauge invariance, Bose symmetry, and CP-conservation [45]:

$$\mathcal{M} = \epsilon_{1\mu}\epsilon_{2\nu} \left[A(x_1, x_2) T_{(1)}^{\mu\nu} + \frac{B(x_1, x_2)}{m_\eta^2} T_{(2)}^{\mu\nu} \right],$$

where $A(x_1, x_2)$ and $B(x_1, x_2)$ are Lorentz-invariant form factors, which are symmetric functions of dimensionless variables

$$x_1 = \frac{p \cdot k_1}{m_\eta^2}, \quad x_2 = \frac{p \cdot k_2}{m_\eta^2}.$$

Two independent gauge-invariant tensors are defined as

$$T_{(1)}^{\mu\nu} = k_2^\mu k_1^\nu - k_1 \cdot k_2 g^{\mu\nu},$$

$$T_{(2)}^{\mu\nu} = k_1 \cdot p k_2^\mu p^\nu + k_2 \cdot p p^\mu k_1^\nu - k_1 \cdot k_2 p^\mu p^\nu - k_1 \cdot p k_2 \cdot p g^{\mu\nu}.$$

If CP is not conserved two more gauge-invariant structures containing $\epsilon_{\mu\nu\lambda\sigma}$ (pseudo)tensor appear [55]. However we can safely neglect tiny effects associated with additional form factors.

The decay width is given by the standard expression

$$d\Gamma = \frac{\delta(p - q - k_1 - k_2)}{16 (2\pi)^5 m_\eta} \sum_{\epsilon_1 \epsilon_2} |\mathcal{M}|^2 \frac{d\vec{q}}{E_\pi} \frac{d\vec{k}_1}{E_1} \frac{d\vec{k}_2}{E_2}. \quad (6)$$

It is straightforward to perform summation over photon polarizations and obtain

$$\begin{aligned} \sum_{\epsilon_1 \epsilon_2} |\mathcal{M}|^2 = \frac{1}{2} m_\eta^4 \left\{ \left| A(x_1, x_2) + \frac{1}{2} B(x_1, x_2) \right|^2 \left[2(x_1 + x_2) + \frac{m_\pi^2}{m_\eta^2} - 1 \right]^2 + \right. \\ \left. \frac{1}{4} |B(x_1, x_2)|^2 \left[4x_1 x_2 - 2(x_1 + x_2) - \frac{m_\pi^2}{m_\eta^2} + 1 \right]^2 \right\}. \end{aligned}$$

Then the decay width is given by the integral

$$\Gamma(\eta \rightarrow \pi^0 \gamma \gamma) = \frac{1}{2!} \frac{m_\eta}{64\pi^3} \int_{x_1^-}^{x_1^+} dx_1 \int_{x_2^-}^{x_2^+} dx_2 \sum_{\epsilon_1 \epsilon_2} |\mathcal{M}|^2,$$

where the integration limits are

$$x_1^- = 0, \quad x_1^+ = \frac{1}{2} \left(1 - \frac{m_\pi^2}{m_\eta^2} \right), \quad x_2^- = \frac{1}{2} \left(1 - 2x_1 - \frac{m_\pi^2}{m_\eta^2} \right)$$

and

$$x_2^+ = \frac{1}{2(1 - 2x_1)} \left(1 - 2x_1 - \frac{m_\pi^2}{m_\eta^2} \right).$$

We need some model to calculate $A(x_1, x_2)$ and $B(x_1, x_2)$ form factors and proceed further. As was already mentioned in the introduction, vector meson exchange $\eta \rightarrow V^* \gamma \rightarrow \pi^0 \gamma \gamma$ gives the most significant contribution. The corresponding form factors have the following form [44]

$$\begin{aligned} A_{VDM}(x_1, x_2) = \\ - \sum_{V=\rho, \omega, \phi} g_{V\eta\gamma} g_{V\pi\gamma}^* \left\{ \frac{1 - x_1}{1 - 2x_1 - \frac{M_V^2}{m_\eta^2}} + \frac{1 - x_2}{1 - 2x_2 - \frac{M_V^2}{m_\eta^2}} \right\}, \\ B_{VDM}(x_1, x_2) = \\ \sum_{V=\rho, \omega, \phi} g_{V\eta\gamma} g_{V\pi\gamma}^* \left\{ \frac{1}{1 - 2x_1 - \frac{M_V^2}{m_\eta^2}} + \frac{1}{1 - 2x_2 - \frac{M_V^2}{m_\eta^2}} \right\}. \end{aligned}$$

In the model considered in [44], which we choose as the base for our Monte Carlo simulation, scalar meson exchange $\eta \rightarrow \pi^0 a_0^* \rightarrow \pi^0 \gamma \gamma$ contribution was also taken into account. If a_0 is considered as a point-like source of photon emission then only $A(x_1, x_2)$ form factor acquires additional contribution from this mechanism

$$A_{a_0}(x_1, x_2) = \frac{g_{a\eta\pi} g_{a\gamma\gamma}}{m_a^2 - m_\eta^2 \left[2(x_1 + x_2) + \frac{m_\pi^2}{m_\eta^2} - 1 \right]}.$$

For the coupling constants we take their central values from Ref.[44], where they were extracted from the experimental information on various decay widths. The relative sign of the VDM and a_0 exchange amplitudes cannot be determined this way. We have chosen constructive interference between them because the experimental width is larger than VDM prediction.

The following resulting values were used in the simulation:

$$\begin{aligned} m_\eta^2 g_{\rho\eta\gamma} g_{\rho\pi\gamma}^* &= 0.0495, & m_\eta^2 g_{\omega\eta\gamma} g_{\omega\pi\gamma}^* &= 0.0294, \\ m_\eta^2 g_{\phi\eta\gamma} g_{\phi\pi\gamma}^* &= 0.00267, & g_{a\eta\pi} g_{a\gamma\gamma} &= 0.0132. \end{aligned}$$

As a check of the simulation program, we reproduced the result of Ref.[44] for the decay width $\Gamma(\eta \rightarrow \pi^0 \gamma \gamma)_{VDM+a_0} = 0.36$ eV.

Equation (6) can be rewritten in a form more convenient for simulation. The δ -function (or energy-momentum conservation) enables us to perform a trivial integration over $d\vec{q}$ and $d\cos\theta_2$ (where θ_2 is the angle between \vec{k}_1 and \vec{k}_2 3-vectors) and get in the η -meson rest frame:

$$d\Gamma = \frac{m_\eta}{64\pi^3} \sum_{\epsilon_1 \epsilon_2} |\mathcal{M}|^2 dx_1 dx_2 \frac{d\cos\theta_1}{2} \frac{d\varphi_1}{2\pi} \frac{d\varphi_2}{2\pi}. \quad (7)$$

x_1, x_2 which were defined earlier, in the η -meson rest frame coincide with photon energies divided by η -meson mass. θ_1 and φ_1 are the first photon polar and azimuthal angles in the η meson rest frame and φ_2 is the second photon azimuthal angle in the plane perpendicular to the first photon momentum \vec{k}_1 . In fact the integrand in (7) after taking into account the energy-momentum conservation depends only on x_1 and x_2 . It is convenient, however, to introduce another angular variable instead of x_2 in the following way. Let S^* be a rest frame of the system consisting of π^0 and the second photon. Of course this system moves in the direction opposite to the \vec{k}_1 if initial η decays at rest. For the energy E_* and invariant mass m_* of the $\pi^0 \gamma$ system we get easily

$$E_* = m_\eta(1 - x_1), \quad m_* = m_\eta \sqrt{1 - 2x_1}. \quad (8)$$

Therefore the Lorentz factor of this system is

$$\gamma = \frac{E_*}{m_*} = \frac{1 - x_1}{\sqrt{1 - 2x_1}}. \quad (9)$$

The energy of the second photon E_2^* in the S^* reference frame is uniquely determined by m_* and hence by x_1 :

$$x_2^* = \frac{E_2^*}{m_\eta} = \frac{m_*^2 - m_\pi^2}{2m_\eta m_*} = \frac{1 - 2x_1 - \frac{m_\pi^2}{m_\eta^2}}{2\sqrt{1 - 2x_1}}, \quad (10)$$

but its direction is arbitrary. Let us denote the polar and azimuthal angles (θ_2^* and φ_2^*) of the second photon in S^* as $\varphi_2^* = \varphi_2$ and θ_2^* — as an angle between the velocity 3-vector of the reference frame S^* and the direction of the second photon. The Lorentz transformation relates x_2 and $\cos \theta_2^*$ in the following way

$$x_2 = \gamma x_2^* (1 + \beta \cos \theta_2^*), \quad \beta = \frac{\sqrt{\gamma^2 - 1}}{\gamma}.$$

Therefore we can rewrite (7) as

$$d\Gamma = \frac{m_\eta}{64\pi^3} f(x_1) \sum_{\epsilon_1 \epsilon_2} |\mathcal{M}|^2 dx_1 \frac{d \cos \theta_1}{2} \frac{d\varphi_1}{2\pi} \frac{d \cos \theta_2^*}{2} \frac{d\varphi_2^*}{2\pi}, \quad (11)$$

where

$$f(x_1) = \frac{dx_2}{d \cos \theta_2^*} = \beta \gamma x_2^* = \sqrt{\gamma^2 - 1} x_2^*.$$

Having equation (11) at hand, we can generate $\eta \rightarrow \pi^0 \gamma \gamma$ decay in the η meson rest frame by the following algorithm:

- generate first photon normalized energy x_1 as a random number uniformly distributed from 0 to x_1^+ . Calculate (π^0, γ) -system energy, mass and the Lorentz factor according to equations (8) and (9).
- generate a random number φ_* uniformly distributed in the interval $[0, 2\pi]$ and take it as the azimuthal angle of the S^* velocity vector in the η meson rest frame, which will be called laboratory frame below. Generate another uniform random number in the interval $[-1, 1]$ and take it as a $\cos \theta_*$, θ_* being the polar angle of the S^* velocity vector in the laboratory frame. This defines the unit vector $\vec{n} = (\sin \theta_* \cos \varphi_*, \sin \theta_* \sin \varphi_*, \cos \theta_*)$ along S^* velocity.

- now the first photon 4-momentum in the laboratory frame can be constructed: $E_1 = m_\eta x_1$, $\vec{k}_1 = -E_1 \vec{n}$.
- generate in the analogous manner φ_2^* and $\cos \theta_2^*$, construct the unit vector \vec{n}^* along the second photon velocity in the S^* frame:

$$\vec{n}^* = (\sin \theta_2^* \cos \varphi_2^*, \sin \theta_2^* \sin \varphi_2^*, \cos \theta_2^*).$$

- calculate x_2^* according to (10) and construct the second photon 4-momentum in the S^* frame: $E_2^* = x_2^* m_\eta$, $\vec{k}_2^* = E_2^* \vec{n}^*$.
- construct the π^0 meson 4-momentum in the S^* frame: $E_\pi^* = m_\pi - E_2^*$, $\vec{q}_\pi^* = -\vec{k}_2^*$.
- construct the π^0 meson and second photon 4-momenta in the laboratory frame from their 4-momenta in the frame S^* by using appropriate Lorentz transformations.
- for generated x_1 and x_2 , calculate

$$z = f(x_1) \sum_{\epsilon_1 \epsilon_2} |\mathcal{M}|^2.$$

- generate a random number z_R uniformly distributed in the interval from 0 to z_{max} , where z_{max} is some number majoring z . That is for all $\eta \rightarrow \pi^0 \gamma \gamma$ decay configurations (for all acceptable values of x_1 and x_2) we should have $z < z_{max}$. In our program we had used $z_{max} = 1.8 \times 10^{-5}$.
- if $z \geq z_R$, accept the event, that is the generated 4-momenta of the π^0 meson and both photons. Otherwise repeat the whole procedure.

Note that equation (11) indicates that the decay width can be calculated by using the above described Monte Carlo algorithm according to

$$\Gamma(\eta \rightarrow \pi^0 \gamma \gamma) = \frac{1}{2!} \frac{m_\eta}{64\pi^3} \left\langle f(x_1) \sum_{\epsilon_1 \epsilon_2} |\mathcal{M}|^2 \right\rangle (x_1^+ - x_1^-),$$

where $\langle \dots \rangle$ stands for the mean value. As another check of the program, we had reproduced the result of [44] for the width by this method also.

To understand whether model dependence of the $\eta \rightarrow \pi^0 \gamma \gamma$ decay matrix element can bring a dangerous systematics in our experimental study of this decay, we performed another Monte Carlo simulation of this process using

significantly different form factors of the quark-box model from [45]. These form factors are reproduced below (in the units of GeV^{-2}):

$$\begin{aligned} & \left[2(x_1 + x_2) + \frac{m_\pi^2}{m_\eta^2} - 1 \right] A_{QB}(x_1, x_2) \approx \\ & -0.616 + 2.14(x_1 + x_2) - 2.509(x_1^2 + x_2^2) - 4.184x_1x_2 + \\ & 1.5896(x_1^3 + x_2^3) + 2.936x_1x_2(x_1 + x_2), \\ B_{QB}(x_1, x_2) \approx & -0.866 + 1.674(x_1 + x_2) - 3.26(x_1^2 + x_2^2) - \\ & 1.781x_1x_2 + 2.37(x_1^3 + x_2^3) + 1.089x_1x_2(x_1 + x_2). \end{aligned}$$

For the quark-box model, we had used $z_{max} = 4.37 \times 10^{-5}$ as majoring value in our Monte Carlo program. The prediction of this model for the decay width is about two times higher than the VDM prediction and is closer to the present experimental result. But this model is also more ambiguous. Its predictions strongly depend on the assumed values for the u and d constituent quark masses (the above given form factors correspond to $m_u = m_d = 300$ MeV). It was proven that in the chiral symmetry limit baryon loop contribution strictly vanishes [29, 30]. In order to check whether quark-box diagram contribution is indeed dominant we must consider other quark-loop diagrams also in the framework of some self-consistent model (for example ENJL model) with realistically broken chiral symmetry. Therefore we took VDM as a basis for our Monte Carlo simulation and used the quark-box model only for systematic error estimation.

4 Data analysis and results

A primary selection of the candidate events for the process

$$e^+e^- \rightarrow \phi \rightarrow \eta\gamma; \eta \rightarrow \pi^0\gamma\gamma \quad (12)$$

was done according to following criteria:

- an event must have no charged particles and contain exactly 5 photons in the calorimeter;
- the azimuthal angle of any final photon lies within the interval $27^\circ < \theta < 153^\circ$;

- the energy of the next to the most energetic photon is less than $0.8E$, E being a beam energy;
- the total energy deposition of final photons is in the range $0.8 \leq E_{tot}/2E \leq 1.1$;
- the normalized full momentum of the event ($P_{tot}/2E$) is less than 0.1;

The third condition is against QED background $e^+e^- \rightarrow 2\gamma$, with extra photons originating either from the beam background or splitting of electromagnetic showers in the calorimeter. The two latter conditions eliminate the main part of the background from the $\phi \rightarrow K_L K_S$ decay.

For the events which passed the primary selection criteria a kinematic fit was performed assuming energy-momentum conservation and the presence of a π^0 meson in an intermediate state. χ^2 of this fit (χ_π) can be used to suppress the most dangerous background from

$$e^+e^- \rightarrow \eta\gamma; \quad \eta \rightarrow 3\pi^0 . \quad (13)$$

In particular the $\chi_\pi < 10$ condition being used in our event selection procedure reduces the background (13) by a factor of two. Another $\sim 20\%$ reduction of this background was achieved by demanding that any photon pair not involving photons from the π^0 meson found by the kinematic fit has an invariant mass outside $m_{\pi^0} \pm 30$ MeV interval.

Another significant background left after the selection criteria described above comes from the process

$$e^+e^- \rightarrow \pi^0\omega \rightarrow \pi^0\pi^0\gamma . \quad (14)$$

This background is only slightly ($\sim 15\%$) reduced by the $\chi_\pi < 10$ cut but is suppressed by an order of magnitude after the invariant masses of photon pairs are restricted as described above to exclude the presence of a second π^0 meson.

To further reduce this background, special kinematic fit was applied to the selected events assuming $\omega\pi^0$ intermediate state. Only the events for which this kinematic fit fails were selected for further analysis.

One more background source is the $e^+e^- \rightarrow 3\gamma$ reaction (both pure QED and $\phi \rightarrow \eta\gamma, \eta \rightarrow 2\gamma$ decay) with extra background photons. These extra photons are usually soft. To suppress this background, a 3γ -kinematic fit was performed under assumption that two photons in the event were spurious. All 3γ -combinations were examined and one with the best χ^2

(denoted as $\chi_{3\gamma}$) was selected. The $e^+e^- \rightarrow 3\gamma$ background is efficiently suppressed by the condition $\chi_{3\gamma} > 20$, while the process (12) itself is only marginally effected.

As was already mentioned, transverse energy profile of the shower enables us to recognize merged photons and additionally suppress the background (13). The corresponding parameter ξ_γ is described in [54]. Fig.5 shows distributions over the parameter ξ_γ for simulated signal events (12) and background (13). The efficiency of this parameter in the background suppression is clearly demonstrated by this figure. We require $\xi_\gamma < -5$ which reduces background (13) by about six times.

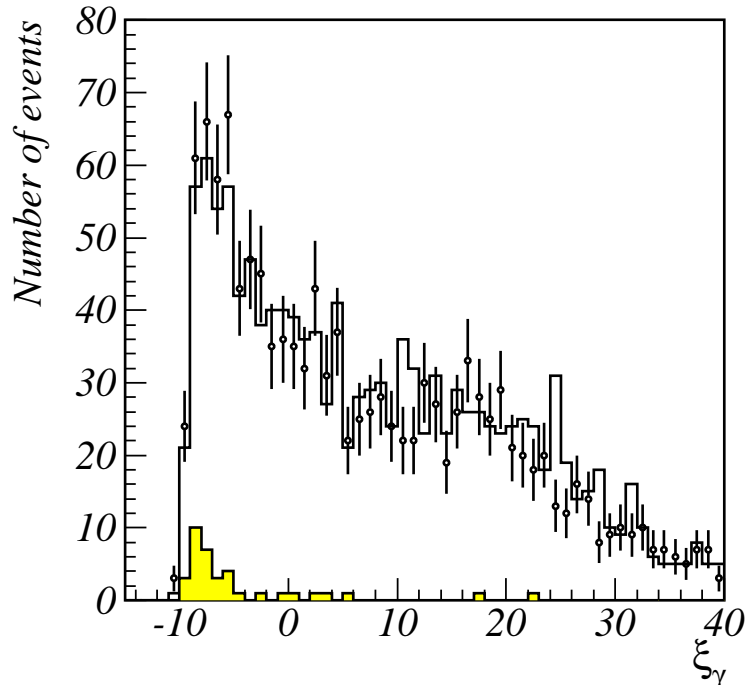


Figure 5: ξ_γ distributions. Histogram — simulated background (13) normalized to experimental statistics. Points with error bars — experiment. Shaded histogram — expected $\eta \rightarrow \pi^0\gamma\gamma$ signal according to simulation of the process (12).

Fig.5 also shows that almost all background remaining after our cuts comes from the process (13). In particular the background from the reaction (14) seems to become insignificant after application of described above selection criteria. But unfortunately it is very difficult to suppress the background (13) any further without significant improvement of the detector performance (angular and energy resolution for photons). So the only option left for us is to subtract the remaining background (13) relying upon the Monte Carlo simulation.

For this purpose, special kinematic fit was performed for selected events. It was assumed in the fit that four of five photons in each event are from the $\eta \rightarrow \pi^0 \gamma \gamma$ decay. Of course there are many possibilities how to divide five photons into the recoil photon from the $\phi \rightarrow \eta \gamma$ decay, two photons from the subsequent $\eta \rightarrow \pi^0 \gamma \gamma$ decay, and two photons from the $\pi^0 \rightarrow \gamma \gamma$ decay. The best combination was selected for each event during the fit. χ^2 of the fit ($\chi_{\pi\gamma\gamma}$) is small for desired events from (12), while background (13) has wider distribution. Fig.6 shows $\chi_{\pi\gamma\gamma}$ distribution for 170 experimental events left after the above described cuts with one more condition $\chi_{\pi\gamma\gamma} < 40$. The simulated background from the process (13) has similar distribution over this parameter.

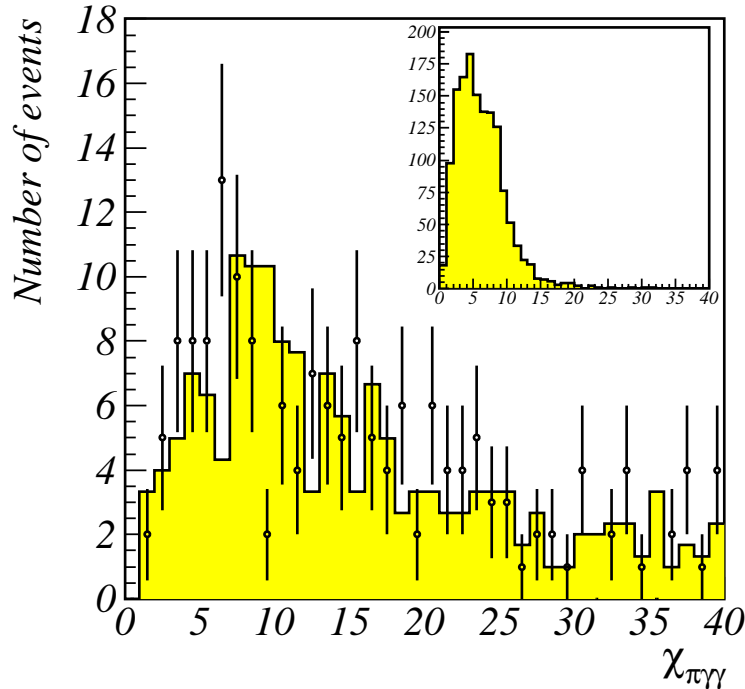


Figure 6: $\chi_{\pi\gamma\gamma}$ distribution. Points with error bars — experiment. Shaded histogram corresponds to the simulated background (13), normalized to experimental statistics. Insertion shows the distribution for simulated $\eta \rightarrow \pi^0 \gamma \gamma$ events.

Signal and background composition of our data sample was estimated by using binned maximum likelihood method incorporating the finiteness of the Monte Carlo statistics [56]. Using HMCMLL routine from the HBOOK package [57], the experimental histogram was fitted by the sum of two Monte Carlo histograms for the signal (12) and background (13). As a result of this fit, the signal events fraction in the experimental data, depicted in Fig.6, was found to be $(4.1 \pm 7.6)\%$. This corresponds to the total number of

signal events of the process (12) $N_S = 7.0_{-6.5}^{+12.9}$, where the asymmetric errors correspond to the 68.27% confidence interval determined according to Table 10 from [58]. Number of background events from this fit $N_B = 163 \pm 19$ is in a good agreement with the prediction of simulation 158.3 ± 11.5 .

To transform N_S into the branching ratio, we need a detection efficiency for signal events. This efficiency determined from simulation of the effect with VDM matrix element is $\epsilon = (14.1 \pm 0.4)\%$. The quark-box matrix element gives almost the same value $\epsilon = (14.8 \pm 0.4)\%$. Therefore the systematic error coming from model ambiguity is negligible in comparison with the inaccuracy in the background subtraction. The Monte Carlo detection efficiency was corrected for a loss of events due to additional beam background photons causing signal events to be rejected by the selection cut requiring exactly 5 photons in an event. This effect not modelled in the simulation was as large as 5% in the first SND experiment and 8% in the second one with a twice larger statistics. Thus as an average corrected detection efficiency for signal events we took $\epsilon = (13.1 \pm 0.8)\%$ with the model ambiguity also taken into account.

The number of η mesons in our initial data sample is 2.58×10^5 with a 3% systematic error due to limited accuracy of the luminosity determination. Given above values for N_S and ϵ we get the branching ratio

$$Br(\eta \rightarrow \pi^0 \gamma \gamma) = (2.1_{-1.9}^{+3.8}) \times 10^{-4}. \quad (15)$$

Since the error is very large only an upper limit of the branching ratio can be determined from our data:

$$Br(\eta \rightarrow \pi^0 \gamma \gamma) < 8.4 \times 10^{-4} \text{ (90\% C.L.)}, \quad (16)$$

where we have again used Table 10 from [58], according to which the measured mean of 0.54σ implies 90% C.L. interval $\mu < 2.18\sigma$ for the mean μ of a Gaussian constrained to be non-negative.

The systematic error caused mainly by inaccuracy of the simulated ξ_γ -distribution was estimated to be less than 20% which is negligible in comparison with the statistical error.

5 Final remarks

Our investigation once more clearly demonstrates experimental difficulties in $\eta \rightarrow \pi^0 \gamma \gamma$ decay studies caused mainly by the background (13). Our

analysis yields the value of the $\eta \rightarrow \pi^0 \gamma \gamma$ branching ratio (with systematic error not greater than 20%) $Br(\eta \rightarrow \pi^0 \gamma \gamma) = (2.1_{-1.9}^{+3.8}) \times 10^{-4}$ which is consistent with a more accurate result of GAMS [16, 17]: $Br(\eta \rightarrow \pi^0 \gamma \gamma) = (7.1 \pm 1.4) \times 10^{-4}$, but shows an urgent need of new high precision measurements. As a final result we present an upper limit:

$$Br(\eta \rightarrow \pi^0 \gamma \gamma) < 8.4 \times 10^{-4} \text{ at } 90\% \text{ C.L.},$$

leaving open the question whether ChPT has problems with this decay. Nevertheless, we think that the investigation presented in this paper demonstrates feasibility of such studies in future high statistics collider experiments. Let us remind in this respect that η mesons will be copiously produced at ϕ -factories, for example, about 10^8 $\phi \rightarrow \eta \gamma$ decays per year are expected at DAΦNE [59]. We hope that this article will stimulate future investigations at ϕ -factories and will be useful in such studies.

acknowledgement

This work is supported in part by Russian Fund for Basic Researches, grant No. 00-15-96802.

References

- [1] G. Di Giugno et al., Phys. Rev. Lett. **16**, (1966) 767.
- [2] M. A. Wahlig, E. Shibata and I. Mannelli, Phys. Rev. Lett. **17**, (1966) 221.
- [3] M. Feldman et al., Phys. Rev. Lett. **18**, (1967) 868.
- [4] C. Baltay et al., Phys. Rev. Lett. **19**, (1967) 1495.
- [5] S. Buniatov et al., Phys. Lett. **25B**, (1967) 560.
- [6] F. Jacquet et al., Phys. Lett. **25B**, (1967) 574.
- [7] F. Jacquet, U. Nguyen-Khac, A. Haatuft and A. Halsteinslid, Nuovo Cimento **63A**, (1969) 743.
- [8] B. Cox, L. Fortney and J. Colson, Phys. Rev. Lett. **24**, (1970) 534.

- [9] M. T. Buttram, M. N. Kreisler and R. E. Mischke, Phys. Rev. Lett. **25**, (1970) 1358.
- [10] S. Devons et al., Phys. Rev. **D1**, (1970) 1936.
- [11] S. Schmitt et al., Phys. Lett. **32B**, (1970) 638.
- [12] Z. S. Strugalski et al., Nucl. Phys. **B27**, (1971) 429.
- [13] A. T. Abrosimov et al., Yad. Fiz. **31**, (1980) 371; Sov. J. Nucl. Phys. **31**, (1980) 195.
- [14] F. Binon et al., Yad. Fiz. **33**, (1981) 1534; Lett. Nuovo Cim. **32**, (1981) 45.
- [15] F. Binon et al., Yad. Fiz. **36**, (1982) 670; Nuovo Cimento **71A**, (1982) 497. Yu. D. Prokoshkin, Yad. Fiz. **62**, (1999) 396; Phys. Atom. Nucl. **62**, (1999) 356.
- [16] D. Alde et al., Yad. Fiz. **40**, (1984) 1447; Z. Phys. **C25**, (1984) 225; L. G. Landsberg, Phys. Rep. **128**, (1985) 301.
- [17] Review of particle Physics, Eur. Phys. J. **C3**, (1998) 360.
- [18] S. Okubo and B. Sakita, Phys. Rev. Lett. **11**, (1963) 50.
- [19] W. Alles, A. Baracca and A. T. Ramos, Nuovo Cimento **A45**, (1966) 272.
- [20] M. Gell-Mann, D. Sharp and W. G. Wagner, Phys. Rev. Lett. **8**, (1962) 261. L. M. Brown and P. Singer, Phys. Rev. Lett. **8**, (1962) 460.
- [21] P. Singer, Phys. Rev. **154**, (1967) 1592.
- [22] G. Oppo and S. Oneda, Phys. Rev. **160**, (1967) 1397.
- [23] G. J. Gounaris, Phys. Rev. **D2**, (1970) 2734.
- [24] M. P. Gokhale, S. H. Patil and S. D. Rindani, Phys. Rev. **D14**, (1976) 2250.
- [25] G. K. Greenhut and G. W. Intemann, Phys. Rev. **D16**, (1977) 776.
- [26] S. Chakrabarty, A. N. Mitra and I. Santhanam, Phys. Lett. **B84**, (1979) 119.

- [27] J. Gasser, H. Leutwyler, Nucl. Phys. **B250**, (1985) 465; Annals Phys. **158**, (1984) 142. For recent review see H. Leutwyler, Chiral dynamics, hep-ph/0008124. A. Pich, Rept. Prog. Phys. **58**, (1995) 563.
- [28] D. Diakonov, V. Petrov, Nucleons as chiral solitons. hep-ph/0009006.
- [29] N. D. Hari Dass, Phys. Rev. **D7**, (1973) 1458.
- [30] M. K. Volkov and D. Ebert, Sov. J. Nucl. Phys. **30**, (1979) 736; Yad. Fiz. **30**, (1979) 1420.
- [31] A. N. Ivanov and N. I. Troitskaya, Yad. Fiz. **36**, (1982) 494.
- [32] M. K. Volkov and D. V. Kreopalov, Sov. J. Nucl. Phys. **37**, (1983) 770; Yad. Fiz. **37**, (1983) 1297.
- [33] L. Ametller, J. Bijnens, A. Bramon and F. Cornet, Phys. Lett. **B276**, (1992) 185.
- [34] C. Picciotto, Nuovo Cimento **A105**, (1992) 27.
- [35] M. Jetter, Nucl. Phys. **B459**, (1996) 283.
- [36] P. Ko, Phys. Rev. **D47**, (1993) 3933.
- [37] P. Ko, Phys. Lett. **B349**, (1995) 555.
- [38] S. Bellucci and C. Bruno, Nucl. Phys. **B452**, (1995) 626.
- [39] A. A. Belkov, A. V. Lanyov and S. Scherer, J. Phys. **G22**, (1996) 1383.
- [40] J. Bijnens, A. Fayyazuddin and J. Prades, Phys. Lett. **B379**, (1996) 209.
- [41] Y. Nemoto, M. Oka and M. Takizawa, Phys. Rev. **D54**, (1996) 6777; Phys. Rev. **D55**, (1997) 4083; Austral. J. Phys. **50**, (1997) 187.
- [42] L. M. Sehgal, Phys. Rev. **D38**, (1988) 808. A. Pich, Rare kaon decays. hep-ph/9610243.
- [43] T. P. Cheng, Phys. Rev. **162**, (1967) 1734.
- [44] N. Ng and D. J. Peters, Phys. Rev. **D46**, (1992) 5034.
- [45] J. N. Ng and D. J. Peters, Phys. Rev. **D47**, (1993) 4939.
- [46] J. Bijnens, Goldstone Boson Production and Decay. hep-ph/9710341.

- [47] A. N. Skrinsky, *in* Proc. of Workshop on physics and detectors for DAΦNE. (Frascati, 1995). Frascati physics series vol. 4, p. 3.
- [48] M.N. Achasov et al., Nucl. Instrum. Meth. **A449**, (2000) 125.
- [49] M.N. Achasov et al., *in* proc. VIII International Conference on Calorimetry in High Energy Physics, (Lisbon, 1999), p. 105. hep-ex/9907038.
- [50] D. A. Bukin et al., Nucl. Instrum. Meth. **A384**, (1997) 360.
D. A. Bukin et al., Nucl. Instrum. Meth. **A379**, (1996) 545.
- [51] M. N. Achasov et al., Nucl. Instrum. Meth. **A401**, (1997) 179.
- [52] M. N. Achasov et al., Nucl. Instrum. Meth. **A411**, (1998) 337.
- [53] M. G. Bekishev and V. N. Ivanchenko, Nucl. Instrum. Meth. **A361**, (1995) 138.
- [54] A. V. Bozhenok, V. N. Ivanchenko and Z. K. Silagadze, Nucl. Instrum. Meth. **A379**, (1996) 507.
- [55] G. Ecker, A. Pich and E. de Rafael, Nucl. Phys. **B303**, (1988) 665.
- [56] R. Barlow and C. Beeston, Comp. Phys. Comm. **77**, (1993) 219.
- [57] HBOOK Reference Manual, Version 4.23, p. 141. (CERN Geneva, 1995).
- [58] G. J. Feldman and R. D. Cousins, Phys. Rev. **D57**, (1998) 3873.
- [59] L. Ametller, *in* The second DAΦNE physics handbook, vol. 1, p. 427. (Frascati, 1995).